Molecular Pharmacology Fast Forward. Published on November 29, 2012 as doi:10.1124/mol.112.083006

Allosteric Modulation of a Chemogenetically Modified G Protein-Coupled Receptor

Alaa Abdul-Ridha, J. Robert Lane, Patrick M. Sexton, Meritxell Canals and Arthur Christopoulos

Drug Discovery Biology, Monash Institute of Pharmaceutical Sciences and

Department of Pharmacology, Monash University, Parkville, Victoria, 3052, Australia.

Molecular Pharmacology Fast Forward. Published on November 29, 2012 as DOI: 10.1124/mol.112.083006
This article has not been copyedited and formatted. The final version may differ from this version.

Running Title: Allosterism at a chemogenetically modified receptor.

Address correspondence to:

Prof. Arthur Christopoulos Drug Discovery Biology

Monash Institute of Pharmaceutical Sciences

Monash University

399 Royal Parade, Parkville, Victoria 3052, Australia.

Phone: (03) 9903 9067

Fax :(03) 9903 9581

Email: arthur.christopoulos@monash.edu

Text pages: 40

Number of tables: 4

Number of figures: 6

Number of references: 38

Number of words in Abstract: 201

Number of words in Introduction: 658

Number of words in discussion: 1378

Molecular Pharmacology Fast Forward. Published on November 29, 2012 as DOI: 10.1124/mol.112.083006
This article has not been copyedited and formatted. The final version may differ from this version.

Abbreviations: mAChR, muscarinic acetylcholine receptor; GPCR, G protein-coupled receptor; ACh, acetylcholine; CNS, central nervous system; BQCA, benzyl quinolone carboxylic acid; DREADD, Designer Receptor Exclusively Activated by Designer Drug; WT, wild type; CNO, clozapine-n-oxide; MWC, Monod-Wyman-Changeux; CHO, chinese hamster ovary; FBS, foetal bovine serum; PBS, phosphate-buffered saline; DMEM, Dulbecco's modified Eagle's medium; QNB, quinuclidinyl benzilate; IP_1, inositolphosphate-1; GppNHp, guanosine 5'-[β, γ-imido] triphosphate; pERK1/2, phosphorylated extracellular signal-regulated kinase; NDMC, n-desmethyl-clozapine; McN-A-343, 4-*I*-[3-chlorophenyl]carbamoyloxy)-2-butynyltrimethylammnonium chloride; TBPB, 1-[1'-(2-methylbenzyl)- 1,4'-bipiperidin-4-yl]-1,3-dihydro-2*H*-benzimidazol-2-one; IBMX, 3-isobutyl-1-methylxanthine; HTRF, homogeneous time resolved FRET; RASSL, receptor activated solely by synthetic ligand; FRET, fluorescence resonance energy transfer.

Molecular Pharmacology Fast Forward. Published on November 29, 2012 as DOI: 10.1124/mol.112.083006
This article has not been copyedited and formatted. The final version may differ from this version.

Abstract

DREADDs (Designer Receptors Exclusively Activated by Designer Drugs) are chemogenetically modified muscarinic acetylcholine receptors (mAChRs) that have minimal responsiveness to acetylcholine (ACh), but are potently and efficaciously activated by an otherwise inert synthetic ligand, clozapine-N-oxide (CNO). DREADDs have been used as tools for selectively modulating signal transduction pathways *in vitro* and *in vivo.* Recent comprehensive studies have validated how the pharmacology of a CNO-bound DREADD mirrors that of an ACh-bound wild-type (WT) mAChR. However, nothing is known about whether this equivalence extends to the allosteric modulation of DREADDs by small molecules. To address this, we investigated the actions at an M_1 DREADD of BQCA, a positive allosteric modulator of ACh binding and function that is known to behave according to a simple two-state mechanism at the WT receptor. We found that allosteric modulation of the CNO-bound DREADD receptor is not equivalent to the corresponding modulation of the ACh-bound WT receptor. We also found that BQCA engenders stimulus bias at the M_1 DREADD, having differential types of cooperativity depending on the signaling pathway. Furthermore, the modulation of ACh itself by BQCA at the DREADD is not compatible with the two state model that we have previously applied to the M_1 WT receptor.

Molecular Pharmacology Fast Forward. Published on November 29, 2012 as DOI: 10.1124/mol.112.083006
This article has not been copyedited and formatted. The final version may differ from this version.

Introduction

Over the last decade, chemical-genetic strategies have been applied in the generation of tools for investigating G protein-coupled receptor (GPCR) function with increasing degrees of spatial and temporal specificity. Such chemogenetically modified GPCRs include receptors activated solely by synthetic ligands (RASSLs) (Pei et al., 2008) and designer receptors exclusively activated by designer drugs (DREADDs) (Armbruster et al., 2007), the latter having been specifically generated using the muscarinic acetylcholine receptor (mAChR) subtypes as the model system (Armbruster et al., 2007). These mAChR DREADDs contain two mutations of conserved orthosteric site residues (Y106C and A196G in the M_1 mAChR) that cause a loss of responsiveness to the cognate agonist, acetylcholine (ACh), whilst engendering the ability to be potently activated by the otherwise biologically inert ligand, clozapine-n-oxide (CNO). When these mutant GPCRs are expressed in a particular tissue, the resultant biological effects observed after administration of CNO only reflect the activation of the chosen DREADD in that particular tissue. As such, DREADDs have proven to be valuable biological tools and have been expressed transgenically to investigate specific functions of several mAChRs and the physiological consequences of their activation *in vivo* (Alexander et al., 2009; Ferguson et al., 2011; Garner et al., 2012; Guettier et al., 2009; Krashes et al., 2011; Ray et al., 2011; Sasaki et al., 2011).

Recently, it has become apparent that different ligands binding to the same GPCR can stabilise specific receptor conformations that are coupled to distinct functional outcomes; a phenomenon termed ‘stimulus bias’, ‘biased agonism’, or ‘functional

Molecular Pharmacology Fast Forward. Published on November 29, 2012 as DOI: 10.1124/mol.112.083006
This article has not been copyedited and formatted. The final version may differ from this version.

selectivity' (Stallaert et al., 2011). This begs the question as to how much the action of the CNO-bound DREADD truly reflects that of the ACh-bound WT receptor. Fortunately, a recent rigorous investigation of multiple signalling and receptor regulatory pathways at the M_3 DREADD concluded that the results obtained from the transgenic expression of the DREADD when activated by CNO are indeed likely to mirror the actions of ACh at the WT receptor (Alvarez-Curto et al., 2011). However, there exist alternative possible utilities of DREADDs for which such vital equivalence with the WT remains undetermined; these possibilities involve the potential combination of DREADDs with small molecule allosteric modulators of GPCRs. As we have previously shown using the M_4 DREADD, it is possible to use an allosteric modulator to 're-activate' the DREADD to its cognate agonist, ACh (Nawaratne et al., 2008). A potential advantage of this approach is that the temporal specificity associated with endogenous ACh release and uptake can be retained while activating the DREADD in a spatially controlled fashion. Irrespective, the nature of allosteric modulation of CNO itself at a DREADD remains unknown, even though this approach may also be considered as a means to better understand GPCR allostery in a tissue/pathway-targeted manner.

An ideal requirement for addressing these issues would be an allosteric modulator that behaves in a predictable manner and does not promote stimulus bias when tested against ACh at a WT mAChR. We have recently characterized the actions of such a ligand, benzyl quinolone carboxylic acid (BQCA), at the M_1 WT mAChR (Canals et al., 2012). Specifically, BQCA displays simple receptor 'state dependence', exhibiting positive cooperativity with orthosteric agonists but negative cooperativity with inverse agonists in a manner that correlates with orthosteric ligand

Molecular Pharmacology Fast Forward. Published on November 29, 2012 as DOI: 10.1124/mol.112.083006
This article has not been copyedited and formatted. The final version may differ from this version.

efficacy. Importantly, the allosteric modulation of BQCA did not engender stimulus-bias at a variety of M_1 mAChR-linked signaling pathways (Canals et al., 2012). The discovery of such a molecule thus presents an unprecedented opportunity to investigate the nature of allosteric modulation of a DREADD with regards to both the cognate receptor agonist, as well as the synthetic activator CNO. Herein, we provide a comprehensive analysis of the allosteric interaction of BQCA with ACh, CNO and a diverse range of M_1 mAChR ligands at multiple downsteam signalling pathways linked to the M_1 WT and DREADD mAChRs. We reveal that allosteric modulation of the CNO-bound DREADD receptor is not equivalent to the ACh-bound WT receptor, and that BQCA engenders stimulus bias at the M_1 DREADD.

Molecular Pharmacology Fast Forward. Published on November 29, 2012 as DOI: 10.1124/mol.112.083006
This article has not been copyedited and formatted. The final version may differ from this version.

Materials and Methods

Materials. Chinese Hamster Ovary (CHO) FlpIn cells and Dulbecco's modified Eagle's medium (DMEM) were purchased from Invitrogen (Carlsbad, CA). Foetal bovine serum (FBS) was purchased from ThermoTrace (Melbourne, Australia). Hygromycin-B was purchased from Roche (Germany). [^{3}H]quinuclidinyl benzilate ([^{3}H]QNB; specific activity, 50 Ci/mmol), cAMP AlphaScreen beads, AlphaScreen reagents and Ultima gold scintillation liquid were purchased from PerkinElmer Life Sciences (Boston, MA). The *Sure-Fire* cellular ERK1/2 assay kits were a generous gift from TGR BioSciences (Adelaide, Australia). IP-One assay kit and reagents were purchased from Cisbio (Codolet, France). Fluo-4-AM was purchased from Molecular Probes (Carlsbad, CA). All other chemicals were purchased from Sigma Aldrich (St.Louis, MO). Benzyl quinolone carboxylic acid (BQCA) was synthesised in house at the Monash Institute of Pharmaceutical Sciences.

Cell culture and receptor mutagenesis. The M_1 DREADD mutations (Y106C/A196G - 3.33 and 5.46, respectively, using the Ballesteros-Weinstein numbering system (Ballesteros and Weinstein, 1995)) were generated using the QuickChange Site-Directed Mutagenesis kit (Agilent Technologies, La Jolla, CA), following the manufacturer's instructions. CHO FlpIn cells stably expressing the M_1 wild type (WT) or DREADD mAChRs were generated and maintained as described previously (Avlani et al., 2010).

Membrane preparation and radioligand binding. Membranes from CHO FlpIn cells stably expressing either M_1 WT or DREADD mAChRs were prepared as

Molecular Pharmacology Fast Forward. Published on November 29, 2012 as DOI: 10.1124/mol.112.083006
This article has not been copyedited and formatted. The final version may differ from this version.

described previously (Nawaratne et al., 2008). Radioligand binding assays were performed using 5µg and 20µg of M_1 WT and DREADD mAChR membrane homogenates, respectively. Membranes were incubated in 1mL binding buffer (20 mM HEPES, 100 mM NaCl, 10 mM, $MgCl_2$, pH 7.4) containing 100µM guanosine 5'-[β, γ-imido] triphosphate (GppNHp) and increasing concentrations of the competing ligand for 1 hour at 37°C in the presence of a fixed concentration of [^{3}H]QNB. Homologous competition binding assays were initially performed to determine the equilibrium dissociation constant of [^{3}H]QNB and the number of binding sites at both M_1 WT and DREADD mAChRs (K_i and B_{max} , respectively). The concentration of [^{3}H]QNB used in all subsequent heterologous competition binding assays was approximately equal to its equilibrium dissociation constant at the M_1 WT mAChR (0.13±0.03 nM; n=3). Interaction studies were performed in the absence or presence of increasing concentrations of BQCA. For all experiments, total and non-specific binding was defined by the absence of competing ligand and the presence of 100µM atropine, respectively. The termination of the assay and measurements of bound radioactivity were performed as described in (Avlani et al., 2010).

Extracellular signal-regulated kinase 1/2 phosphorylation assays. Assays to measure M_1 mAChR-mediated stimulation of ERK1/2 phosphorylation were performed using the AlphaScreen-based SureFire™ kit (TGR Biosciences, Australia), following the manufacturer's instructions. Briefly, FlpIn CHO cells stably expressing either the M_1 WT or DREADD mAChRs were seeded into 96-well culture plates at 40,000 cells per well and allowed to adhere. Cells were then rinsed with PBS and serum starved overnight at 37°C, 5% CO_2. The following day, cells were stimulated with agonist. Initial ERK1/2 phosphorylation (pERK1/2) time-course

Molecular Pharmacology Fast Forward. Published on November 29, 2012 as DOI: 10.1124/mol.112.083006
This article has not been copyedited and formatted. The final version may differ from this version.

experiments were performed to determine the time of maximal ERK1/2 phosphorylation for each agonist (found to be 5 min for all agonists tested). The time of peak agonist response was then used for the establishment of concentration-response curves. For functional interaction studies, cells were incubated at 37°C with varying concentrations of agonist in the absence and presence of varying concentrations of BQCA, which was co-added with the agonist. In all experiments, 10% (v/v) FBS was used as positive control of pERK1/2. The reaction was terminated by removal of media and addition of lysis buffer. Samples were processed according to kit instructions. The fluorescence signal was measured using a Fusion-α plate reader (PerkinElmer Life Sciences, Boston, MA). Data were normalised to the maximum response elicited by 10% (v/v) FBS at the same time point.

Intracellular Ca^{2+} mobilization assays. FlpIn CHO cells were seeded at 35,000 cells per well into 96-well culture plates and allowed to grow overnight at 37°C, 5% CO_2. Cells were washed twice with Ca^{2+} assay buffer (150mM NaCl, 2.6mM KCl, 1.2mM $MgCl_2$, 10mM D-Glucose, 10mM HEPES, 2.2mM $CaCl_2$, 0.5% (w/v) BSA and 4mM probenecid) pH 7.4 and incubated in Ca^{2+} assay buffer containing 1μM Fluo-4-AM for 1 hour in the dark at 37°C 5% CO_2. After two washes with Ca^{2+} assay buffer, fluorescence was measured for 1.5 min upon the addition of agonist (or co-addition of agonist and BQCA) in a Flexstation (Molecular Devices, Sunnyvale, CA) using an excitation wavelength of 485nm and emission wavelength of 520nm. Data were normalised to the peak response elicited by 2μM ionomycin.

Molecular Pharmacology Fast Forward. Published on November 29, 2012 as DOI: 10.1124/mol.112.083006
This article has not been copyedited and formatted. The final version may differ from this version.

cAMP accumulation assays. FlpIn CHO cells were seeded at 35,000 cells per well into 96-well culture plates and allowed to grow overnight at 37°C, 5% CO_2. Cells were incubated with 90µl of stimulation buffer (phenol red-free DMEM containing 0.1% (w/v) BSA, 5mM HEPES, 0.5mM 3-isobutyl-1-methylxanthine (IBMX)) pH 7.4 for 30 min at 37°C, 5% CO_2. Cells were stimulated with agonist for 30min after which the media was removed and cells were precipitated with 100% ethanol. Ethanol was allowed to evaporate at room temperature or in a non-humidified incubator at 37°C. After ethanol evaporation, cells were lysed with lysis buffer (0.3% Tween20, 5mM HEPES, 0.1% (w/v) BSA). Lysates were processed according to the AlphaScreen kit manufacturer instructions (PerkinElmer Life Sciences, Boston, MA). The fluorescence signal was measured using a Fusion-α plate reader (PerkinElmer Life Sciences, Boston, MA). Data were normalised to the maximum response elicited by 100µM forskolin.

IP -One accumulation assays. Inositol Phosphate-1 (IP_1) was measured using the IPOne assay kit (Cisbio, France), following the manufacturer's instructions. Briefly, FlpIn CHO cells were seeded into 384-well proxy-plates at 7,500 cells per well and allowed to grow overnight at 37°C, 5% CO_2. The following day cells were stimulated with agonists in IP_1 stimulation buffer (in the absence or presence of BQCA) and incubated for 1h at 37°C, 5% CO_2. IP_1-d2 and anti–IP_1-cryptate were prepared in IP_1 lysis buffer and incubated with the cells for 1h at room temperature. Homogeneous time resolved FRET (HTRF) was measured in an Envision plate reader (PerkinElmer Life Sciences, Boston, MA). Values for each sample were extrapolated from the IP_1 standard curve and data were normalised to the maximum control response.

Molecular Pharmacology Fast Forward. Published on November 29, 2012 as DOI: 10.1124/mol.112.083006
This article has not been copyedited and formatted. The final version may differ from this version.

Data Analysis. All data were analysed using Prism 5.0 (GraphPad Software, San Diego, CA). Inhibition binding curves between [^{3}H]QNB and unlabelled ligands were fitted to a one site binding model (Motulsky H, 2004). BQCA binding-interaction studies were fitted to the following allosteric ternary complex model (Ehlert, 1988): (equation 1)

$$Y = \frac{Bmax[A]}{[A] + \left(\frac{K_A K_B}{\alpha'[B] + K_B}\right)\left(1 + \frac{[I]}{K_I} + \frac{[B]}{K_B} + \frac{\alpha[I][B]}{K_I K_B}\right)} \qquad (1)$$

where Y is percentage (vehicle control) binding, Bmax is the total number of receptors, [A], [B] and [I] are the concentrations of [^{3}H]QNB, BQCA and the orthosteric ligand, respectively, K_A and K_B and K_I are the equilibrium dissociation constants of [^{3}H]QNB, BQCA and the orthosteric ligand, respectively. α' and α are the binding cooperativities between BQCA and [^{3}H]QNB, and BQCA the orthosteric ligand, respectively. Values of α (or α')>1 denote positive cooperativity; values <1 (but >0) denote negative cooperativity, and values =1 denote neutral cooperativity.

Concentration-response curves for the interaction between BQCA and the orthosteric ligand in the various functional signalling assays were globally fitted to the following operational model of allosterism and agonism (Leach et al., 2007): (equation 2)

$$E = \frac{E_m(\tau_A[A](K_B + \alpha\beta[B]) + \tau_B[B]K_A)^n}{([A]K_B + K_A K_B + [B]K_A + \alpha[A][B])^n + (\tau_A[A](K_B + \alpha\beta[B]) + \tau_B[B]K_A)^n} \qquad (2)$$

where E_m is the maximum possible cellular response, [A] and [B] are the concentrations of orthosteric and allosteric ligands, respectively, K_A and K_B are the equilibrium dissociation constant of the orthosteric and allosteric ligands, respectively, τ_A and τ_B are operational measures of orthosteric and allosteric ligand efficacy (which incorporate both signal efficiency and receptor density), respectively, α is the binding cooperativity parameter between the orthosteric and allosteric ligand, and β denotes the magnitude of the allosteric effect of the modulator on the efficacy of the orthosteric agonist. In all instances, the equilibrium dissociation constant of each agonist was fixed to that determined from the binding assays. All affinity, potency, and cooperativity values are estimated as logarithms (Christopoulos, 1998) and statistical comparisons between values were by Student's *t* test. A value of $P<0.05$ was considered statistically significant.

Molecular Pharmacology Fast Forward. Published on November 29, 2012 as DOI: 10.1124/mol.112.083006
This article has not been copyedited and formatted. The final version may differ from this version.

Results

Pharmacological characterisation of the M_1 WT and M_1 DREADD mAChR.

To characterise the pharmacology of the M_1 DREADD in comparison to that of the M_1 WT mAChR, the binding and activation profiles of a range of ligands were examined (Supplemental Figure 1). Using [^{3}H]QNB as a prototypical orthosteric antagonist, we performed equilibrium homologous competition binding studies in membrane preparations of CHO FlpIn cells stably expressing the M_1 WT or M_1 DREADD mAChRs. The DREADD displayed a significant reduction in the affinity of [^{3}H]QNB (pK_A = 8.23 ± 0.06; n=3, P<0.05) when compared to the WT (pK_A = 9.88 ± 0.12; n = 3) consistent with previous findings for DREADDs (Armbruster et al., 2007; Nawaratne et al., 2008). The receptor expression level of the M_1 DREADD was not significantly different from the WT receptor (B_{max} = 4.90 ± 0.35 vs 5.10 ± 0.12 pmol/mg of protein for WT and DREADD receptors, respectively). Subsequent testing of structurally diverse ligands in equilibrium binding studies using 0.13nM [^{3}H]QNB revealed different effects of the DREADD mutations on ligand binding depending on the nature of the ligand studied (Fig.1, Table 1 and Supplemental Figure 2). The affinities of the endogenous orthosteric agonist, ACh and the partial agonist xanomeline were significantly reduced at the M_1 DREADD (Fig.1, Table 1, Supplemental Figure 1 and Supplemental Figure 2). In contrast, the affinities of clozapine, its metabolite N-desmethylclozapine (NDMC), and the synthetic analogue CNO, were significantly enhanced at the M_1 DREADD. Interestingly, TBPB and McN-A-343, which may have a 'bitopic' (dual allosteric/orthosteric) mode of interaction at the mAChRs (Valant et al., 2012b) and display distinct sensitivities to residues proposed to be involved in orthosteric ligand binding (Jacobson et al., 2010;

Molecular Pharmacology Fast Forward. Published on November 29, 2012 as DOI: 10.1124/mol.112.083006
This article has not been copyedited and formatted. The final version may differ from this version.

Valant et al., 2008), showed no significant difference in their binding affinity at the M_1 WT and M_1 DREADD (Table 1, Supplemental Figure1 and Supplemental Figure 2). BQCA itself caused partial inhibition of [^{3}H]QNB binding both at the WT and DREADD M_1 mAChR, consistent with our previous finding of a negative cooperativity with the antagonist and a low affinity for the allosteric site on the free receptor (Canals et al., 2012); estimates of the pK_I value from the current study were 4.15±0.11 and 4.05±0.13 for M_1 WT and DREADD mAChRs, respectively (Fig. 1, Table 1).

We also investigated the ability of the different ligands to activate WT and DREADD receptors using intracellular Ca^{2+} mobilization as a canonical measure of M_1 mAChR activation resulting from preferential coupling to $G\alpha_q$ proteins. Both ACh and xanomeline displayed a significant loss of potency at the M_1 DREADD, while clozapine and its derivatives CNO and NDMC gained potency and/or efficacy at the M_1 DREADD (Fig. 1, Table 1 and Supplemental Figure 3). TBPB activated the M_1 DREADD with comparable potency and efficacy to its activity at the WT receptor. However, in contrast to the unaltered binding profile at the M_1 DREADD, McN-A-343 displayed reduced potency and efficacy at this receptor (Table 1 and Supplemental Figure 3). At the M_1 WT mAChR, BQCA also behaved as a potent and efficacious allosteric agonist in its own right. However, the mutations in the M_1 DREADD caused a significant abolishment in BQCA's action, despite having no effect on its affinity (Fig. 1C and F, Table 1).

Allosteric modulation of CNO binding affinity at the M_1 DREADD is less than that of ACh at the M_1 WT mAChR.

Molecular Pharmacology Fast Forward. Published on November 29, 2012 as DOI: 10.1124/mol.112.083006
This article has not been copyedited and formatted. The final version may differ from this version.

Given the previously determined functional equivalence between CNO at the DREADD and ACh at the WT mAChR (Alvarez-Curto et al., 2011; Armbruster et al., 2007), we investigated whether such equivalence is retained in terms of allosteric modulation. To investigate the effects of BQCA on the affinity of the co-bound ligand, interaction studies were performed between ACh or CNO and varying concentrations of BQCA against a fixed concentration of [^{3}H]QNB (Fig.2). BQCA substantially potentiated ACh-mediated inhibition of equilibrium binding of [^{3}H]QNB at the M_1 WT mAChR (Fig. 2A). A similar pattern of potentiation was observed in the interaction between CNO and BQCA at the M_1 DREADD (Fig. 2D). However, when this potentiation was quantified by application of an allosteric ternary complex model to the data (Equation 1; Table 2), we found that the positive binding cooperativity between ACh and BQCA at the M_1 WT mAChR (α=331) was significantly higher than that with CNO at the M_1 DREADD (α=60). Conversely, BQCA had no effects on the affinity of CNO at the M_1 WT and of ACh at the M_1 DREADD, indicating neutral binding cooperativity (Fig. 2B and C).

The allosteric interaction between ACh and BQCA is consistent with a two-state mechanism at the M_1 WT but not at the M_1 DREADD.

To gain further insight into the functional modulation mediated by BQCA, we performed interaction studies using multiple signalling pathways linked to M_1 mAChR activation, namely; intracellular Ca^{2+} mobilization, ERK1/2 phosphorylation, cAMP and IP_1 accumulation. Figure 3 shows the interaction between ACh and BQCA at both the M_1 WT and DREADD mAChRs in the various signalling pathways. BQCA strongly potentiated the action of ACh at the M_1 WT mAChR, in addition to exhibiting

Molecular Pharmacology Fast Forward. Published on November 29, 2012 as DOI: 10.1124/mol.112.083006
This article has not been copyedited and formatted. The final version may differ from this version.

agonism on its own in the two highly amplified and efficiently coupled signalling pathways, i.e. intracellular Ca^{2+} mobilization and ERK1/2 phosphorylation (Fig. 3A and 3B). In the cAMP accumulation pathway (where stimulus-response coupling efficiency is weak), BQCA's agonism was less pronounced, but robust potentiation of ACh was still evident (Fig 3C). These data were globally fitted to an operational model of allosterism (Equation 2) to yield the parameters shown in Table 3; for this analysis, the binding affinity of BQCA was fixed to the pK_B value determined from the binding studies (Table 1). In agreement with our previous study (Canals et al., 2012), BQCA displayed the highest levels of positive cooperativity (quantified by the operational αβ parameter) at the pathways where the orthosteric agonist exhibited the highest degrees of signalling efficacy (quantified by the operational model τ_A parameter), as would be expected if the allostery was operative within a simple two-state mechanism. However, when analogous interaction studies between ACh and BQCA were performed at the M_1 DREADD, we noted that BQCA robustly enhanced the potency of ACh in both the Ca^{2+} mobilization and pERK1/2 pathways (Fig. 3D and 3E) despite having no effect on ACh binding affinity. Additionally, in experiments measuring stimulation of intracellular cAMP production, where ACh showed no agonistic activity at the DREADD, BQCA was able to partially rescue its signalling efficacy (Fig. 3F). While BQCA displayed high positive cooperativity with ACh at the M_1 DREADD, this cooperativity did not track with the degree of agonist efficacy across the pathways, in contrast to what was observed at the M_1 WT mAChR (Table 3, and see correlation analysis below), suggesting that the two state behaviour of BQCA vs ACh may not be maintained at the M_1 DREADD.

BQCA engenders biased allosteric modulation of CNO at the M_1 DREADD.

Molecular Pharmacology Fast Forward. Published on November 29, 2012 as DOI: 10.1124/mol.112.083006
This article has not been copyedited and formatted. The final version may differ from this version.

Subsequent experiments focused on the functional modulation by BQCA of CNO. In contrast to the large and positive cooperativity seen between ACh and BQCA in the Ca^{2+} mobilization pathway at the M_1 WT mAChR (Fig. 3A and Table 3), BQCA had a minimal effect on the action of CNO at the M_1 DREADD in the same pathway (Fig. 4A). To rule out the possibility that this observation resulted from potential hemi-equilibrium conditions in the Ca^{2+} mobilization assay, we repeated the same experiment in an IP_1 accumulation assay. Again, BQCA did not potentiate the action of CNO in this latter assay (Fig. 4B). Application of the operational model to the data yielded the estimates shown in Table 4. Given that the positive binding cooperativity (α value) between CNO and BQCA was 60, our results suggest that BQCA actually has a *negative* effect on the signalling efficacy of CNO, with estimated values of β= 0.03 and β=0.13 for the Ca^{2+} mobilization and IP_1 assays, respectively. In contrast, BQCA enhanced the action of CNO in the ERK1/2 phosphorylation pathway (Fig. 4C) with a composite cooperativity (αβ) of 41 (Table 4). Given the similar cooperativity estimated from binding studies (α = 60), this indicates the presence of essentially neutral modulation at the level of signalling efficacy (β).

Collectively, as summarized in Figure 5, these findings suggest that BQCA engenders stimulus bias at the M_1 DREADD by demonstrating neutral functional modulation in one pathway (ERK1/2 phosphorylation) and negative functional modulation in another (Ca^{2+} mobilization). Despite the overall large positive cooperativity between BQCA and CNO at the M_1 DREADD in the pERK1/2 pathway, it is still significantly smaller than the cooperativity between ACh and BQCA at both the M_1 WT and DREADD mAChRs in the same signalling pathway. When this interaction was examined in the cAMP pathway, BQCA positively modulated the

Molecular Pharmacology Fast Forward. Published on November 29, 2012 as DOI: 10.1124/mol.112.083006
This article has not been copyedited and formatted. The final version may differ from this version.

potency of CNO but had negative effects on its efficacy (Fig. 4D). This broad spectrum of pharmacological behaviours at the M_1 DREADD indicates that the actions of BQCA do not conform to a simple 'two-state' model, in contrast to its behaviour at the M_1 WT mAChR.

***BQCA consistently conforms to a 'two-state' allosteric model in its interaction with various ligands at the M_1 WT mAChR but not at the M_1 DREADD*.**

To examine if the bias engendered by BQCA at the M_1 DREADD is a result of the receptor conformation stabilised by the co-bound ligand, we explored the interaction of BQCA with various mAChR ligands. We first utilized NDMC, a clozapine metabolite with a similar binding and activation profile to CNO at the M_1 DREADD (Table 1, Supplemental Figure 2E and Supplemental Figure 3E). In the binding interaction studies, BQCA caused a substantial increase in the affinity of NDMC to compete with [^{3}H]QNB. The positive binding cooperativity was estimated to have a value of Log α = 2.15±0.03 (α=141) (Table 2 and Supplemental Figure 4A). Furthermore, the stimulus bias of BQCA at the M_1 DREADD was again demonstrated by its interaction with NDMC in the functional signalling pathways, whereby it displayed negative efficacy modulation of NDMC in the Ca^{2+} mobilization pathway, but neutral modulation of NDMC efficacy in the ERK1/2 phosphorylation pathway (Supplemental Figure 4B and 4C and Supplemental Table 1). Similar to the CNO interaction studies, BQCA caused a reduction in the efficacy of NDMC in the cAMP pathway (Supplemental Figure 4D). These results demonstrate that the biased allosteric behaviour of BQCA at the M_1 DREADD is likely to be resulting from the conformations stabilised by the clozapine derivatives CNO and NDMC at this

Molecular Pharmacology Fast Forward. Published on November 29, 2012 as DOI: 10.1124/mol.112.083006
This article has not been copyedited and formatted. The final version may differ from this version.

receptor, since the same pattern of modulatory bias across signalling pathways at the M_1 DREADD was not observed in the interaction of BQCA with ACh (Fig 3D, 3E and 3F).

Subsequently, we extended these studies to the other mAChR ligands. The data from each ligand-BQCA interaction experiment were globally fitted to the operational model of allosterism (equation 2) and the relationship between the parameters Log τ_A and Log$\alpha\beta$ was examined for each set of ligand interactions (Supplemental Table 2). As shown in Fig. 6, a significant correlation between the parameters Log τ_A and Log$\alpha\beta$ can be observed at the M_1 WT mAChR in both the Ca^{2+} mobilization (Pearson's r^2= 0.736; p=0.01) and pERK1/2 pathways (Pearson's r^2=0.625; p=0.03), providing further evidence for the allosteric two-state behaviour of BQCA at this receptor. When the same set of ligand-BQCA interactions studies were performed `at the M_1 DREADD and analysed in the same manner, no significant correlation was observed between the parameters Log τ_A and Log$\alpha\beta$ in both the Ca^{2+} mobilization (Pearson's r^2=0.004; p=0.89) and pERK1/2 pathways (Pearson's r^2=0.264; p=0.24). These results therefore suggest that the two-state model proposed for the mechanism of action of BQCA at the WT mAChR is applicable beyond its interaction with ACh, but is not applicable at the M_1 DREADD.

Molecular Pharmacology Fast Forward. Published on November 29, 2012 as DOI: 10.1124/mol.112.083006
This article has not been copyedited and formatted. The final version may differ from this version.

Discussion

Recent studies have provided compelling evidence that the CNO-bound DREADD mAChR retains functional equivalence with the ACh-bound WT mAChR, thus validating the chemogenetically modified DREADD as a powerful tool for probing GPCR signaling in a highly specific manner (Alexander et al., 2009; Alvarez-Curto et al., 2011; Guettier et al., 2009; Krashes et al., 2011). In the current study, we extended this question to the phenomenon of small molecule allostery, and explored the behaviour of BQCA in its interaction with a number of structurally and functionally diverse ligands at the M_1 DREADD. This modulator was chosen because we have recently demonstrated that its actions at the M_1 WT mAChR can be reconciled within a two-state receptor model, akin to that applied to many ion channels, thus representing the simplest case of allosteric modulation with clear, predictable properties (Canals et al., 2012). We reveal that allosteric modulation of the CNO-bound DREADD receptor is not equivalent to the corresponding modulation of the ACh-bound WT receptor. In addition, we find that BQCA engenders stimulus bias at the M_1 DREADD, most strikingly by behaving as a neutral allosteric modulator of CNO efficacy in the pERK1/2 pathway while having negative modulation in the Ca^{2+} mobilization and IP_1 pathways. Moreover, the modulation of ACh itself by BQCA at the DREADD is also not compatible with a simple two state model that we have applied to the M_1 WT. These findings indicate that the behavior of the DREADD with respect to allosteric modulation is a manifestation of multiple, distinct, receptor conformations.

Molecular Pharmacology Fast Forward. Published on November 29, 2012 as DOI: 10.1124/mol.112.083006
This article has not been copyedited and formatted. The final version may differ from this version.

Because mAChR subtypes are characterised by a very high degree of amino acid sequence conservation within the orthosteric (ACh) binding site (Wess et al., 2003), previous attempts to target the M_1 mAChR have failed due to unwanted side-effects that result from their lack of subtype selectivity (Conn et al., 2009). An alternative approach to achieve subtype selectivity is to develop ligands that target allosteric sites that are less conserved between subtypes (Christopoulos, 2002). BQCA is one such compound that has high subtype selectivity for the M_1 mAChR. Importantly, the modulator exhibits both *in vitro* and *in vivo* efficacy as a potentiator of ACh affinity and signalling (Canals et al., 2012; Ma et al., 2009; Shirey et al., 2009). Allosteric modulators such as BQCA represent not only potential therapeutics, but are also useful tools to study the selective activation of GPCRs both *in vitro* and *in vivo*. Another powerful method for generating tools to study receptor activity in a defined spatial and temporal manner is the chemogenetic approach, as exemplified by the generation of DREADDs (Conklin, 2007). Given the potential offered by the combination of these two approaches to interrogate M_1 mAChR function, it is essential to perform a detailed pharmacological characterization of this mutant receptor. While several studies have transgenically expressed the DREADD receptors in animal models and investigated the physiological consequence of activating them *in vivo* (Alexander et al., 2009; Ferguson et al., 2011; Garner et al., 2012; Guettier et al., 2009; Krashes et al., 2011; Ray et al., 2011; Sasaki et al., 2011), no study has thus far studied allosteric or bitopic ligands at these mutant receptors. By using ACh and xanomeline as orthosteric ligands, TBPB and McN-A-343 as ligands that possibly have a bitopic mode of interaction with the mAChRs (Jacobson et al., 2010; Valant et al., 2008), CNO as the orthosteric ligand at the M_1 DREADD and its analogues clozapine and NDMC, we identified different profiles of

Molecular Pharmacology Fast Forward. Published on November 29, 2012 as DOI: 10.1124/mol.112.083006
This article has not been copyedited and formatted. The final version may differ from this version.

receptor binding and activation at the M_1 DREADD that suggest multiple modes of receptor engagement (Fig. 1 and Table 1, Supplemental Figure 1, Supplemental Figure 2 and Supplemental Figure 3). As expected from prior studies using DREADDs, the affinity and potency of ACh and xanomeline were reduced, while CNO and its structural analogues, NDMC and clozapine, showed significant gains in these parameters. Interestingly, we reveal for the first time that the affinity and potency of TBPB was unaffected by the M_1 DREADD mutations. Unlike TBPB, however, McN-A-343, a partial M_1 mAChR agonist that has been shown to be bitopic at the M_2 mAChR (Valant et al., 2008), displayed reduced potency and efficacy at the M_1 DREADD that was not due to a loss of binding affinity (Table 1, Supplemental Figure 2 and Supplemental Figure 3), indicating that the DREADD mutations had a specific effect on the ability of McN-A-343 to mediate receptor transition into an active state; this appears not to be the case for TBPB.

In addition to providing insights into the nature of putative bitopic ligand interactions on the DREADDs, the key finding of the current study was the consequences of allosteric modulation of both the cognate as well as synthetic agonists in this system. In agreement with our previous study (Canals et al., 2012), BQCA exhibited key hallmarks of allostery within a two-state system at the WT M_1 mAChR, including positive or negative modulation of orthosteric ligand activity depending on the nature of the orthosteric ligand (i.e., positive or inverse agonist), and different strengths of cooperativity depending on the intrinsic efficacy of the orthosteric ligand and the magnitude of stimulus-response coupling of the studied signal pathway. It can, of course, be questioned as to how an allosteric modulator can behave in a manner consistent with a two-state model at GPCRs given that these receptors adopt a

Molecular Pharmacology Fast Forward. Published on November 29, 2012 as DOI: 10.1124/mol.112.083006
This article has not been copyedited and formatted. The final version may differ from this version.

larger spectrum of biologically active states; a prerequisite, in fact, for biased signalling (Mary et al., 2012; Vaidehi and Kenakin, 2010). This can be reconciled within a model whereby the modulator changes the abundance, but not the quality/nature, of different microstates that govern receptor activity; an overall change in abundance of active microstates in one direction relative to 'inactive' microstates would still appear, at a macroscopic level, as a "two-state" system. In contrast, a change in the nature or quality of the microstates, in addition to their abundance, would manifest as biased modulation. In this regard, BQCA is a relatively unique, but extremely useful tool compound, for probing allosteric principles compared to the more complex behaviours of numerous allosteric modulators at different GPCR families that appear to promote pathway-biased modulation to various extents (Davey et al., 2012; Maillet et al., 2007; Marlo et al., 2009; Mathiesen et al., 2005; Stewart et al., 2010; Valant et al., 2012a)

At first glance, it may also be argued that the functional equivalence between ACh at the WT M_1 mAChR and CNO at the M_1 DREADD is retained with regards to the effects of BQCA in a two-state model. Specifically, the higher degree of positive cooperativity between the modulator and ACh at the WT M_1 mAChR, relative to its effects on CNO at the M_1 DREADD, would be expected, given that ACh displays higher efficacy at the WT than CNO at the DREADD (compare, for instance, the $Log\tau_A$ values for ACh at the WT M_1 mAChR in Table 3 to the $Log\tau_A$ values for CNO at the M_1 DREADD in Table 4). However, there were two key lines of evidence arguing against this conformational equivalence with regards to allosteric modulation of the two receptors. First, the degree of cooperativity between various orthosteric

Molecular Pharmacology Fast Forward. Published on November 29, 2012 as DOI: 10.1124/mol.112.083006
This article has not been copyedited and formatted. The final version may differ from this version.

agonists and BQCA at the DREADD did not track with the degree of efficacy displayed by the agonists, which is a key expectation of the two-state model, and is generally evident at the WT M_1 mAChR (Fig. 6). Second, and more strikingly, the interaction between BQCA and CNO at the DREADD was characterized by positive, neutral or negative modulation of CNO efficacy, depending on the pathway being monitored. A similar pattern of BQCA allosteric modulation was observed when the functional interaction studies were performed with NDMC instead of CNO (Supplemental Figure 4 and Supplemental Table 1). These results suggest that the pattern of biased modulation is likely to result from a unique receptor conformation stabilised by clozapine derivatives in combination with BQCA at the M_1 DREADD that is distinct from that stabilized by ACh and BQCA at the M_1 WT mAChR. The recent advances in GPCR (and mAChR particularly) structural biology (Haga et al., 2012; Kruse et al., 2012), together with novel biophysical approaches to study receptor conformations, offer an ideal platform to compare the M_1 WT and M_1 DREADD from a structural perspective and therefore to provide mechanistic insight into the differences observed in our studies

Molecular Pharmacology Fast Forward. Published on November 29, 2012 as DOI: 10.1124/mol.112.083006
This article has not been copyedited and formatted. The final version may differ from this version.

Acknowledgments

We thank Dr. Michael Crouch (TGR Biosciences) for generously providing the ERK1/2 phosphorylation assay kit and Briana J. Davie for the chemical synthesis of BQCA.

Authorship contributions

Participated in research design: *Abdul-Ridha, Lane, Sexton, Canals and Christopoulos*

Conducted experiments: *Abdul-Ridha*

Contributed new reagents or analytical tools: *N/A*

Performed data analysis: *Abdul-Ridha, Lane, Canals and Christopoulos*

Wrote or contributed to writing of the manuscript: *Abdul-Ridha, Lane, Sexton, Canals and Christopoulos*

References

Alexander, G.M., Rogan, S.C., Abbas, A.I., Armbruster, B.N., Pei, Y., Allen, J.A., Nonneman, R.J., Hartmann, J., Moy, S.S., Nicolelis, M.A., McNamara, J.O., and Roth, B.L. (2009). Remote control of neuronal activity in transgenic mice expressing evolved G protein-coupled receptors. Neuron ***63***, 27-39.

Alvarez-Curto, E., Prihandoko, R., Tautermann, C.S., Zwier, J.M., Pediani, J.D., Lohse, M.J., Hoffmann, C., Tobin, A.B., and Milligan, G. (2011). Developing chemical genetic approaches to explore G protein-coupled receptor function: validation of the use of a receptor activated solely by synthetic ligand (RASSL). Mol Pharmacol ***80***, 1033-1046.

Armbruster, B.N., Li, X., Pausch, M.H., Herlitze, S., and Roth, B.L. (2007). Evolving the lock to fit the key to create a family of G protein-coupled receptors potently activated by an inert ligand. Proc Natl Acad Sci U S A ***104***, 5163-5168.

Avlani, V.A., Langmead, C.J., Guida, E., Wood, M.D., Tehan, B.G., Herdon, H.J., Watson, J.M., Sexton, P.M., and Christopoulos, A. (2010). Orthosteric and allosteric modes of interaction of novel selective agonists of the M1 muscarinic acetylcholine receptor. Mol Pharmacol ***78***, 94-104.

Ballesteros, J.A., and Weinstein, H. (1995). [19] Integrated methods for the construction of three-dimensional models and computational probing of structure-function relations in G protein-coupled receptors. In Methods in Neurosciences, C.S. Stuart, ed. (Academic Press), pp. 366-428.

Canals, M., Lane, J.R., Wen, A., Scammells, P.J., Sexton, P.M., and Christopoulos, A. (2012). A Monod-Wyman-Changeux Mechanism Can Explain G Protein-coupled Receptor (GPCR) Allosteric Modulation. J Biol Chem ***287***, 650-659.

Christopoulos, A. (1998). Assessing the distribution of parameters in models of ligand-receptor interaction: to log or not to log. Trends Pharmacol Sci ***19***, 351-357.

Christopoulos, A. (2002). Allosteric binding sites on cell-surface receptors: novel targets for drug discovery. Nat Rev Drug Discov ***1***, 198-210.

Conklin, B.R. (2007). New tools to build synthetic hormonal pathways. Proc Natl Acad Sci USA ***104***, 4777-4778.

Conn, P.J., Jones, C.K., and Lindsley, C.W. (2009). Subtype-selective allosteric modulators of muscarinic receptors for the treatment of CNS disorders. Trends Pharmacol Sci ***30***, 148-155.

Davey, A.E., Leach, K., Valant, C., Conigrave, A.D., Sexton, P.M., and Christopoulos, A. (2012). Positive and Negative Allosteric Modulators Promote Biased Signaling at the Calcium-Sensing Receptor. Endocrinology ***153***, 1232-1241.

Ehlert, F.J. (1988). Estimation of the affinities of allosteric ligands using radioligand binding and pharmacological null methods. Mol Pharmacol ***33***, 187-194.

Ferguson, S.M., Eskenazi, D., Ishikawa, M., Wanat, M.J., Phillips, P.E., Dong, Y., Roth, B.L., and Neumaier, J.F. (2011). Transient neuronal inhibition reveals opposing roles of indirect and direct pathways in sensitization. Nat Neurosci ***14***, 22-24.

Garner, A.R., Rowland, D.C., Hwang, S.Y., Baumgaertel, K., Roth, B.L., Kentros, C., and Mayford, M. (2012). Generation of a Synthetic Memory Trace. Science ***335***, 1513-1516.

Guettier, J.M., Gautam, D., Scarselli, M., Ruiz de Azua, I., Li, J.H., Rosemond, E., Ma, X., Gonzalez, F.J., Armbruster, B.N., Lu, H., Roth, B.L., and Wess, J.

(2009). A chemical-genetic approach to study G protein regulation of beta cell function in vivo. Proc Natl Acad Sci U S A ***106***, 19197-19202.

Haga, K., Kruse, A.C., Asada, H., Yurugi-Kobayashi, T., Shiroishi, M., Zhang, C., Weis, W.I., Okada, T., Kobilka, B.K., Haga, T., and Kobayashi, T. (2012). Structure of the human M2 muscarinic acetylcholine receptor bound to an antagonist. Nature ***482***, 547-551.

Jacobson, M.A., Kreatsoulas, C., Pascarella, D.M., O'Brien, J.A., and Sur, C. (2010). The M1 muscarinic receptor allosteric agonists AC-42 and 1-[1'-(2-methylbenzyl)-1,4'-bipiperidin-4-yl]-1,3-dihydro-2H-benzimidazol- 2-one bind to a unique site distinct from the acetylcholine orthosteric site. Mol Pharmacol ***78***, 648-657.

Krashes, M.J., Koda, S., Ye, C., Rogan, S.C., Adams, A.C., Cusher, D.S., Maratos-Flier, E., Roth, B.L., and Lowell, B.B. (2011). Rapid, reversible activation of AgRP neurons drives feeding behavior in mice. J Clin Invest ***121***, 1424-1428.

Kruse, A.C., Hu, J., Pan, A.C., Arlow, D.H., Rosenbaum, D.M., Rosemond, E., Green, H.F., Liu, T., Chae, P.S., Dror, R.O., Shaw, D.E., Weis, W.I., Wess, J., and Kobilka, B.K. (2012). Structure and dynamics of the M3 muscarinic acetylcholine receptor. Nature ***482***, 552-556.

Leach, K., Sexton, P.M., and Christopoulos, A. (2007). Allosteric GPCR modulators: taking advantage of permissive receptor pharmacology. Trends Pharmacol Sci ***28***, 382-389.

Ma, L., Seager, M.A., Wittmann, M., Jacobson, M., Bickel, D., Burno, M., Jones, K., Graufelds, V.K., Xu, G., Pearson, M., McCampbell, A., Gaspar, R., Shughrue, P., Danziger, A., Regan, C., Flick, R., Pascarella, D., Garson, S., Doran, S., Kreatsoulas, C., Veng, L., Lindsley, C.W., Shipe, W., Kuduk, S., Sur, C.,

Kinney, G., Seabrook, G.R., and Ray, W.J. (2009). Selective activation of the M1 muscarinic acetylcholine receptor achieved by allosteric potentiation. Proc Natl Acad Sci U S A ***106***, 15950-15955.

Maillet, E.L., Pellegrini, N., Valant, C., Bucher, B., Hibert, M., Bourguignon, J.-J., and Galzi, J.-L. (2007). A novel, conformation-specific allosteric inhibitor of the tachykinin NK2 receptor (NK2R) with functionally selective properties. The FASEB Journal ***21***, 2124-2134.

Marlo, J.E., Niswender, C.M., Days, E.L., Bridges, T.M., Xiang, Y., Rodriguez, A.L., Shirey, J.K., Brady, A.E., Nalywajko, T., Luo, Q., Austin, C.A., Williams, M.B., Kim, K., Williams, R., Orton, D., Brown, H.A., Lindsley, C.W., Weaver, C.D., and Conn, P.J. (2009). Discovery and characterization of novel allosteric potentiators of M1 muscarinic receptors reveals multiple modes of activity. Mol Pharmacol ***75***, 577-588.

Mary, S., Damian, M., Louet, M., Floquet, N., Fehrentz, J.A., Marie, J., Martinez, J., and Baneres, J.L. (2012). Ligands and signaling proteins govern the conformational landscape explored by a G protein-coupled receptor. Proc Natl Acad Sci U S A ***109***, 8304-8309.

Mathiesen, J.M., Ulven, T., Martini, L., Gerlach, L.O., Heinemann, A., and Kostenis, E. (2005). Identification of Indole Derivatives Exclusively Interfering with a G Protein-Independent Signaling Pathway of the Prostaglandin D2 Receptor CRTH2. Mol Pharmacol ***68***, 393-402.

Motulsky H, C.A. (2004). Fitting Models to Biological Data Using Linear and Nonlinear Regression. A Practical Guide to Curve Fitting (New York, Oxford University Press).

Nawaratne, V., Leach, K., Suratman, N., Loiacono, R.E., Felder, C.C., Armbruster, B.N., Roth, B.L., Sexton, P.M., and Christopoulos, A. (2008). New insights into the function of M4 muscarinic acetylcholine receptors gained using a novel allosteric modulator and a DREADD (designer receptor exclusively activated by a designer drug). Mol Pharmacol ***74***, 1119-1131.

Pei, Y., Rogan, S.C., Yan, F., and Roth, B.L. (2008). Engineered GPCRs as Tools to Modulate Signal Transduction. Physiology ***23***, 313-321.

Ray, R.S., Corcoran, A.E., Brust, R.D., Kim, J.C., Richerson, G.B., Nattie, E., and Dymecki, S.M. (2011). Impaired Respiratory and Body Temperature Control Upon Acute Serotonergic Neuron Inhibition. Science ***333***, 637-642.

Sasaki, K., Suzuki, M., Mieda, M., Tsujino, N., Roth, B., and Sakurai, T. (2011). Pharmacogenetic modulation of orexin neurons alters sleep/wakefulness states in mice. PLoS One ***6***, e20360.

Shirey, J.K., Brady, A.E., Jones, P.J., Davis, A.A., Bridges, T.M., Kennedy, J.P., Jadhav, S.B., Menon, U.N., Xiang, Z., Watson, M.L., Christian, E.P., Doherty, J.J., Quirk, M.C., Snyder, D.H., Lah, J.J., Levey, A.I., Nicolle, M.M., Lindsley, C.W., and Conn, P.J. (2009). A selective allosteric potentiator of the M1 muscarinic acetylcholine receptor increases activity of medial prefrontal cortical neurons and restores impairments in reversal learning. J Neurosci ***29***, 14271-14286.

Stallaert, W., Christopoulos, A., and Bouvier, M. (2011). Ligand functional selectivity and quantitative pharmacology at G protein-coupled receptors. Expert Opin Drug Discov ***6***, 811-825.

Stewart, G.D., Sexton, P.M., and Christopoulos, A. (2010). Prediction of functionally selective allosteric interactions at an M3 muscarinic acetylcholine receptor mutant using Saccharomyces cerevisiae. Mol Pharmacol ***78***, 205-214.

Vaidehi, N., and Kenakin, T. (2010). The role of conformational ensembles of seven transmembrane receptors in functional selectivity. Curr Opin Pharmacol ***10***, 775-781.

Valant, C., Felder, C.C., Sexton, P.M., and Christopoulos, A. (2012a). Probe dependence in the allosteric modulation of a g protein-coupled receptor: implications for detection and validation of allosteric ligand effects. Mol Pharmacol ***81***, 41-52.

Valant, C., Gregory, K.J., Hall, N.E., Scammells, P.J., Lew, M.J., Sexton, P.M., and Christopoulos, A. (2008). A novel mechanism of G protein-coupled receptor functional selectivity. Muscarinic partial agonist McN-A-343 as a bitopic orthosteric/allosteric ligand. J Biol Chem ***283***, 29312-29321.

Valant, C., Robert Lane, J., Sexton, P.M., and Christopoulos, A. (2012b). The best of both worlds? Bitopic orthosteric/allosteric ligands of g protein-coupled receptors. Annu Rev Pharmacol Toxicol ***52***, 153-178.

Wess, J., Duttaroy, A., Zhang, W., Gomeza, J., Cui, Y., Miyakawa, T., Bymaster, F.P., McKinzie, L., Felder, C.C., Lamping, K.G., Faraci, F.M., Deng, C., and Yamada, M. (2003). M1-M5 muscarinic receptor knockout mice as novel tools to study the physiological roles of the muscarinic cholinergic system. Receptors Channels ***9***, 279-290.

Footnotes

MC and AC contributed equally to this work.

This work was funded by the National Health and Medical Research Council of Australia (NHMRC) [Program Grant 519461] A.C., P.M.S, [Project Grant APP1011796] M.C, and [Project Grant APP1011920] J.R.L. A.C is a Senior, and P.M.S a Principal, Research Fellow of the NHMRC. A.A is a recipient of an Australian Postgraduate Award scholarship.

Molecular Pharmacology Fast Forward. Published on November 29, 2012 as DOI: 10.1124/mol.112.083006
This article has not been copyedited and formatted. The final version may differ from this version.

Figure Legends

Figure 1. Ligand binding and activation properties at the M_1 WT and DREADD mAChRs. The equilibrium binding of the antagonist [^{3}H]QNB was inhibited by (A) ACh, (B) CNO and (C) BQCA in membranes of FlpIn CHO cells expressing the WT M_1 mAChR (closed circles) and M_1 DREADD (open circles). All assays were performed using 0.13nM [^{3}H]QNB in the presence of 100μM GppNHp for 1h at 37°C. Concentration-response curves of intracellular Ca^{2+} mobilization assays were constructed for (D) ACh, (E) CNO and (F) BQCA, in CHO FlpIn cells stably expressing the WT M_1 mAChR (closed circles) and M_1 DREADD (open circles) at 37°C. Data points represent the mean ± S.E. of three independent experiments performed in duplicate. Refer to Table 1 for parameters.

Figure 2. Allosteric modulation of CNO binding affinity at the M_1 DREADD is less than that of ACh at the M_1 WT mAChR.

BQCA potentiated ACh and CNO-mediated inhibition of equilibrium binding of [^{3}H]QNB (A and D) but had no effect on the binding affinity of CNO and ACh (B and C) in membranes of FlpIn CHO cells at the WT M_1 and DREADD mAChRs, respectively. All assays were performed using 0.13nM [^{3}H]QNB in the presence of 100μM GppNHp for 1h at 37°C. Data points represent the mean ± S.E. of three independent experiments performed in triplicate. Curves drawn through the points in A and D represent the best fit of an allosteric ternary complex model (Equation 1; Table 2).

Molecular Pharmacology Fast Forward. Published on November 29, 2012 as DOI: 10.1124/mol.112.083006
This article has not been copyedited and formatted. The final version may differ from this version.

Figure 3. The allosteric interaction between ACh and BQCA is consistent with a two-state mechanism at the M_1 WT but not at the M_1 DREADD. Interaction between BQCA and ACh in intracellular Ca^{2+} mobilization (A and D) ERK1/2 phosphorylation (B and E) or cAMP accumulation (C and F) in CHO FlpIn cells stably expressing the M_1 WT or M_1 DREADD mAChRs. Data points represent the mean ± S.E. of three independent experiments performed in duplicate. Curves drawn through the points represent the best fit of an operational allosteric model (Equation 2; Table 3).

Figure 4. BQCA engenders biased allosteric modulation of CNO at the M_1 DREADD. Interaction between BQCA and CNO in intracellular Ca^{2+} mobilization (A), IP_1 accumulation (B), ERK1/2 phosphorylation (C) and cAMP accumulation (D) in CHO FlpIn cells stably expressing the M_1 DREADD mAChR. Data points represent the mean ± S.E. of three independent experiments performed in duplicate. Curves drawn through the points in A-C represent the best fit of an operational allosteric model (Equation 2; Table 4).

Figure 5. BQCA displays divergent cooperativity estimates with ACh and CNO at the WT M_1 and DREADD mAChRs. Individual estimates of α and β values calculated by subtraction of the cooperativity factors determined in the radioligand binding studies (Fig 2A&D, Table 2) from the composite estimates determined from the functional assays (Fig.3A&B, 4A&C, Table 3&4). * Significantly different ($P<0.05$), two-tailed Students t test, from the corresponding parameter at the WT receptor.

Molecular Pharmacology Fast Forward. Published on November 29, 2012 as DOI: 10.1124/mol.112.083006
This article has not been copyedited and formatted. The final version may differ from this version.

Figure 6. Correlation plots examining the allosteric behaviour of BQCA and its interaction with various ligands at the WT M_1 and DREADD mAChRs. Significant correlation between Log τ_A and Log αβ parameters is observed in BQCA's allosteric interaction with various ligands at the M_1 WT mAChR in both the Ca^{2+} mobilization (A) and ERK1/2 phosphorylation (B) pathways; dashed lines indicate the 95% confidence intervals. No significant correlation can be observed at the M_1 DREADD in the same signalling pathways. Data points represent the operational model parameters (Table S2) for the functional allosteric interactions between BQCA and each of the ligands.

Molecular Pharmacology Fast Forward. Published on November 29, 2012 as DOI: 10.1124/mol.112.083006
This article has not been copyedited and formatted. The final version may differ from this version.

Table 1 [^{3}H]QNB inhibition binding (pK_I) and Ca^{2+} mobilization potency (pEC_{50}) parameters for various ligands at the M_1 WT and DREADD mAChRs. Estimated parameter values represent the mean ± S.E. of three experiments performed in duplicate.

	M_1 WT		M_1 DREADD	
Ligand	**pK_I [a]**	**pEC_{50} [b]**	**pK_I**	**pEC_{50}**
ACh	3.86±0.04	8.54±0.06	2.43±0.07*	3.74±0.12*
Xanomeline	6.84±0.02	8.38±0.06	5.10±0.03*	5.83±0.07*
TBPB	6.76±0.08	7.86±0.10	6.45±0.09	7.30±0.19
McN-A-343	4.71±0.08	7.54±0.05	4.37±0.10	5.39±0.08*
CNO	5.18±0.07	5.95±0.07	5.93±0.04*	8.87±0.07*
Clozapine	6.81±0.07	7.14±0.40	7.93±0.08*	9.30±0.07*
NDMC	6.60±0.05	7.49±0.09	7.40±0.02*	9.33±0.08*
BQCA	4.15±0.11	8.02±0.06	4.05±0.13	4.16±0.16*

a *Negative logarithm of the equilibrium dissociation constant for each ligand.*

b *Negative logarithm of the EC_{50}.*

* *Significantly different (P<0.05), two-tailed Students t test, from the corresponding parameter at the M_1 WT mAChR.*

Molecular Pharmacology Fast Forward. Published on November 29, 2012 as DOI: 10.1124/mol.112.083006
This article has not been copyedited and formatted. The final version may differ from this version.

Table 2 Binding cooperativity parameters for the interaction between [^{3}H]QNB, BQCA and various mAChR ligands at the M_1 WT and DREADD mAChRs. Estimated parameter values represent the mean ± S.E. of three experiments performed in triplicate and analysed according to equation 1.

	M_1 WT	M_1 DREADD
	Log α (α) [a]	Log α (α)
ACh	2.52±0.03 (331)	ND
Xanomeline	ND	ND
TBPB	ND	ND
McN-A-343	1.06±0.07 (11)	ND
CNO	0.64±0.06 (4.5)	1.78±0.05* (60)
Clozapine	ND	1.10±0.14 (13)
NDMC	1.02±0.06 (10.5)	2.15±0.03* (141)

[a] *Logarithm of the binding cooperativity factor between BQCA and the interacting ligand as estimated from Equation 1; antilogarithm shown in parentheses. For this analysis, pK_A was constrained to 9.88 and 8.32, and pK_B was constrained to 4.15 and 4.05 at the M_1 WT and DREADD mAChRs, respectively (Table 1). The cooperativity between BQCA and [^{3}H]QNB was constrained to zero, consistent with high negative cooperativity between the modulator and the radioligand.*

ND *Not determined (no modulation of affinity).*

* *Significantly different (P<0.05), two-tailed Students t test, from the value of ACh at the M_1 WT.*

Molecular Pharmacology Fast Forward. Published on November 29, 2012 as DOI: 10.1124/mol.112.083006
This article has not been copyedited and formatted. The final version may differ from this version.

Table 3 Operational model parameters for the functional allosteric interaction between ACh and BQCA at the M_1 mAChR. Estimated parameter values represent the mean ± S.E of three experiments performed in duplicate and analysed according to equation 2. For this analysis, the pK_B value for BQCA was fixed to that determined from the radioligand binding assays.

	M_1 WT			M_1 DREADD		
	Ca^{2+}	pERK1/2	cAMP	Ca^{2+}	pERK1/2	cAMP
Log τ_A [a]	4.78±0.10	4.71±0.07	1.36±0.16	1.31±0.11	1.53±0.05	ND
Log τ_B [b]	3.19±0.05	2.75±0.03	-0.51±0.30	0.30±0.08	0.28±0.06	ND
(τ_B)	(1550)	(560)	(0.31)	(2)	(2)	
Log αβ [c]	4.10±0.20	3.84±0.17	2.30±0.14	2.92±0.14	2.40±0.07	ND
(αβ)	(12590)	(6918)	(200)	(831)	(251)	

[a] *Logarithm of the operational efficacy parameter of the orthosteric agonist.*

[b] *Logarithm of the operational efficacy parameter of the allosteric agonist.*

[c] *Logarithm of the cooperativity between ACh and BQCA. Antilogarithm shown in parentheses.*

ND not determined.

Molecular Pharmacology Fast Forward. Published on November 29, 2012 as DOI: 10.1124/mol.112.083006
This article has not been copyedited and formatted. The final version may differ from this version.

Table 4 Operational model parameters for the functional allosteric interaction between CNO and BQCA at the M_1 DREADD. Estimated parameter values represent the mean ± S.E from three experiments performed in duplicate and analysed according to equation 2. All other details are as for Table 3.

	Ca^{2+}	pERK1/2	IP_1
Log τ_A	2.81±0.04	2.65±0.10	2.12±0.05
Log τ_B	0.38±0.04	0.44±0.17	0.41±0.07
(τ_B)	(2.4)	(2.8)	(2.6)
Log αβ (αβ)	0.30±0.29 (2)*	1.61±0.22 (41)*	0.88±0.21 (7.5)

** Significantly different (P<0.05), two-tailed Students t test, from the corresponding value at the M_1 WT in Table 3.*

Figure 1

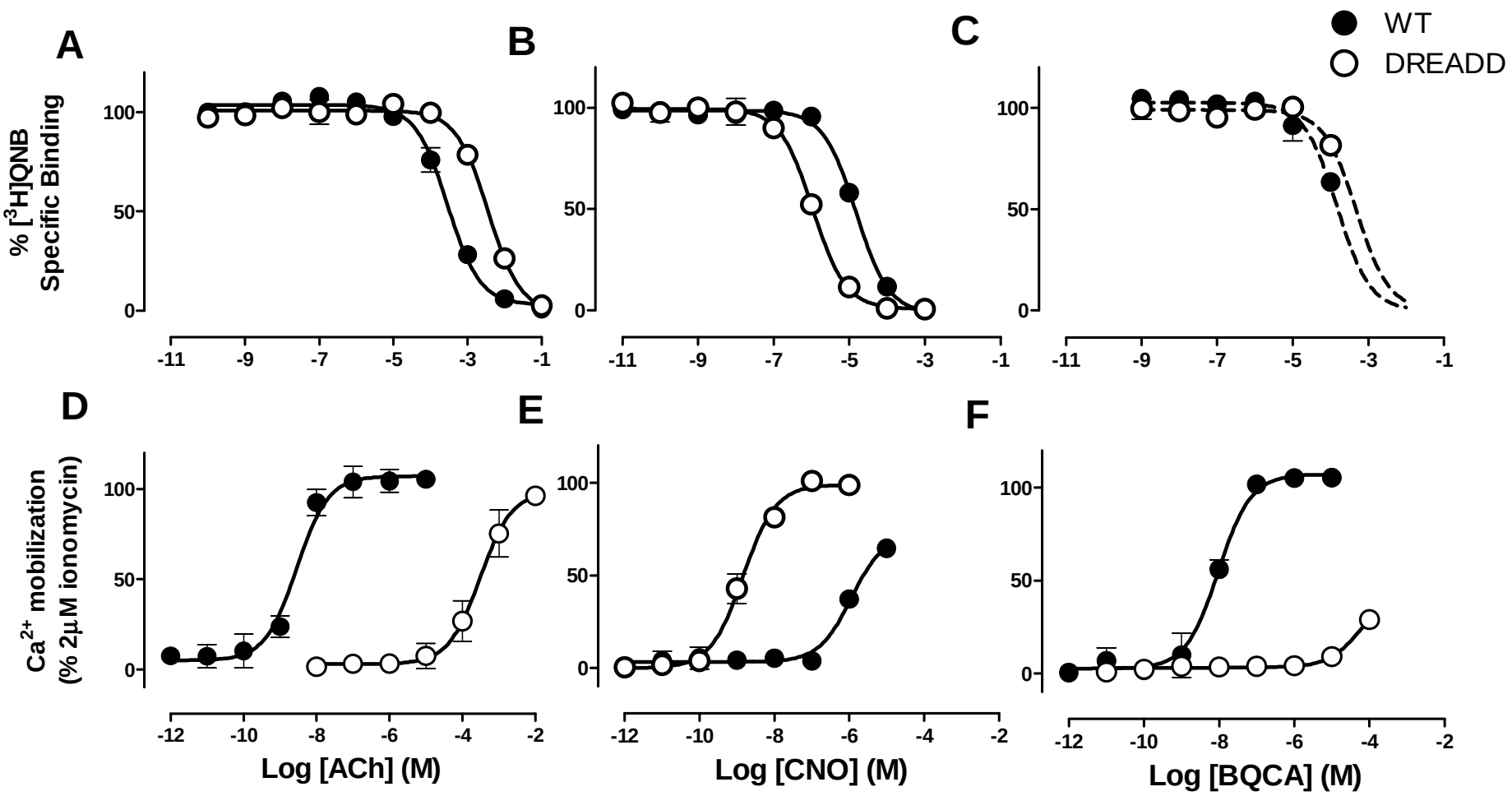

Figure 2

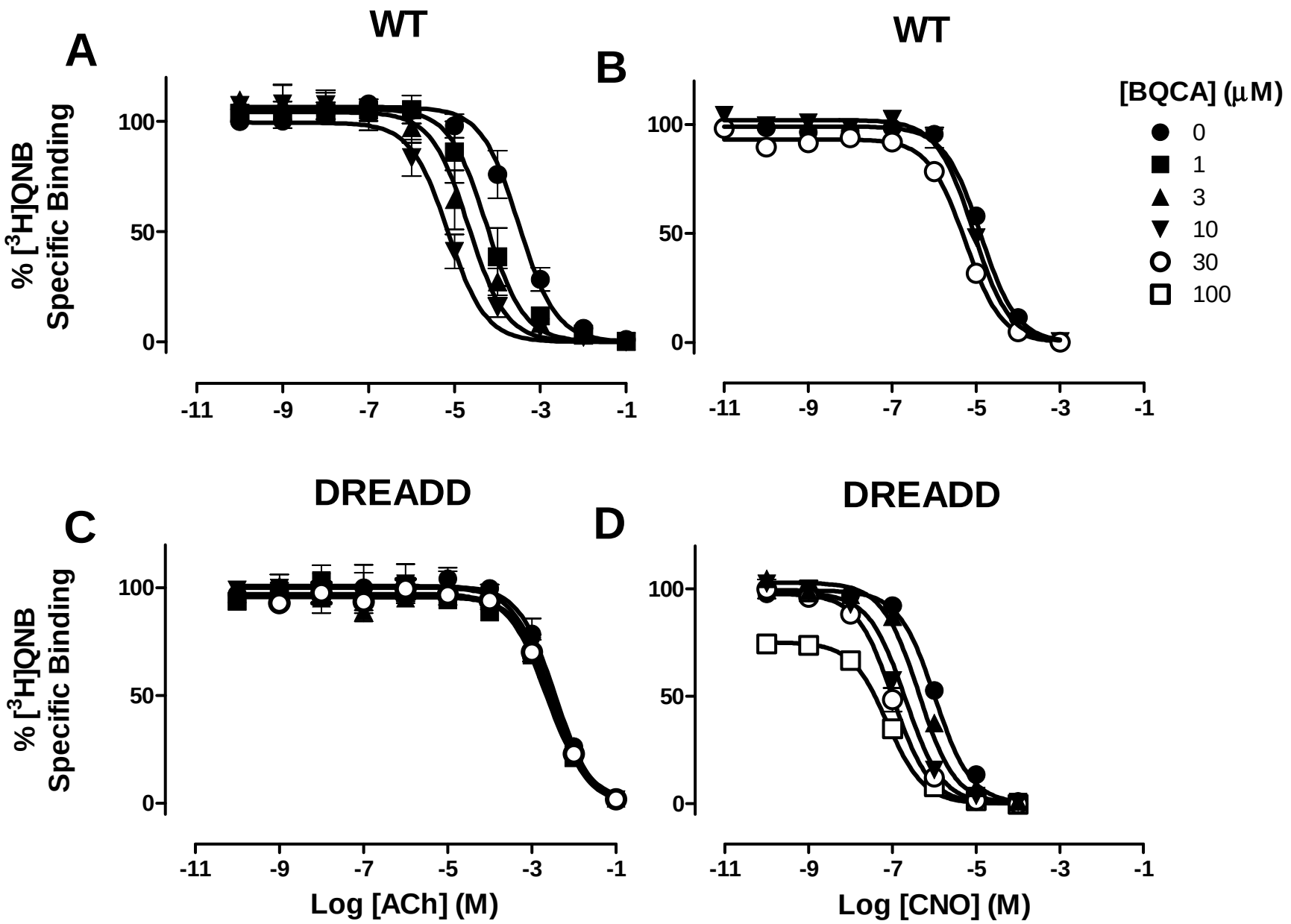

Figure 3

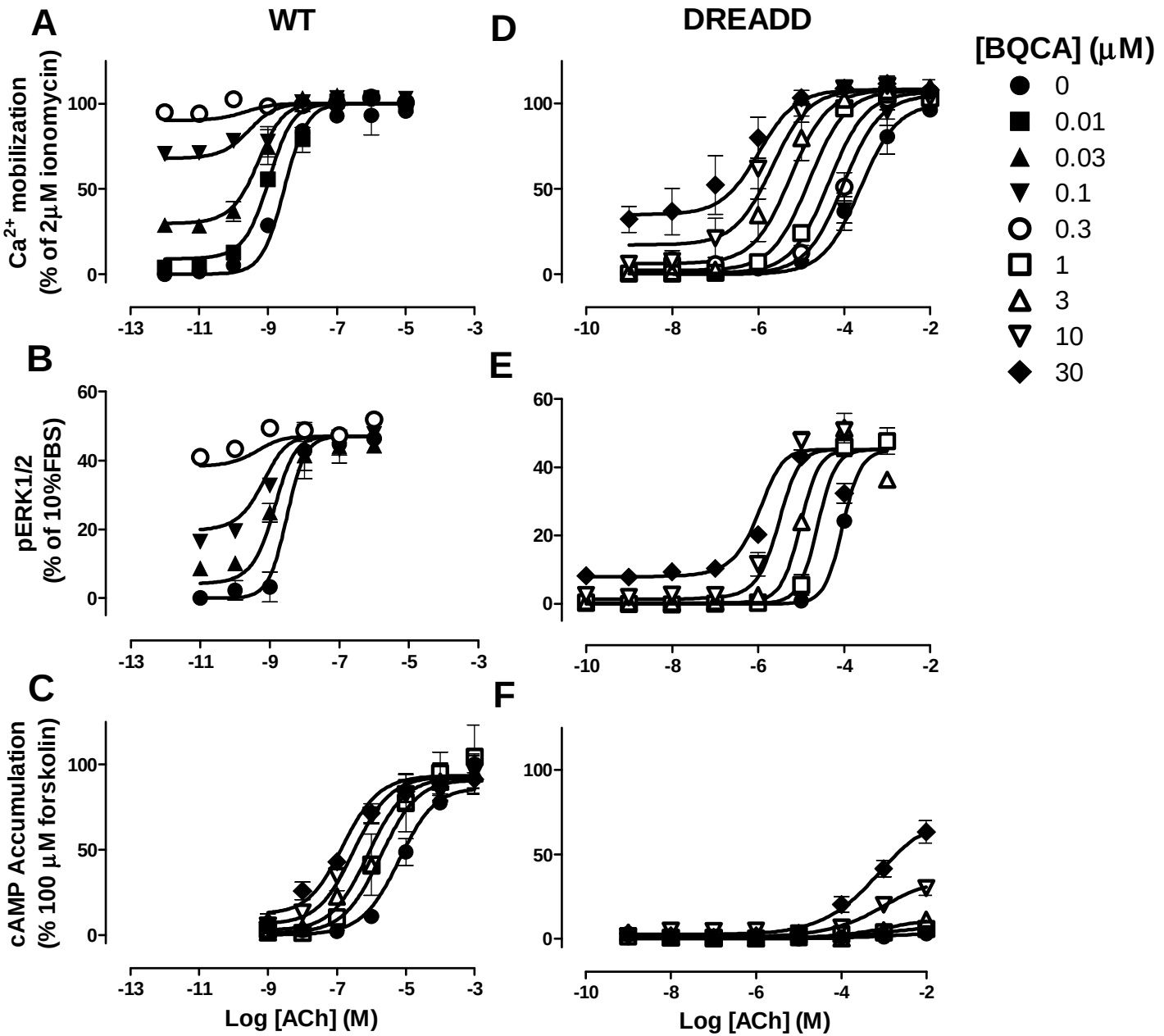

Figure 4

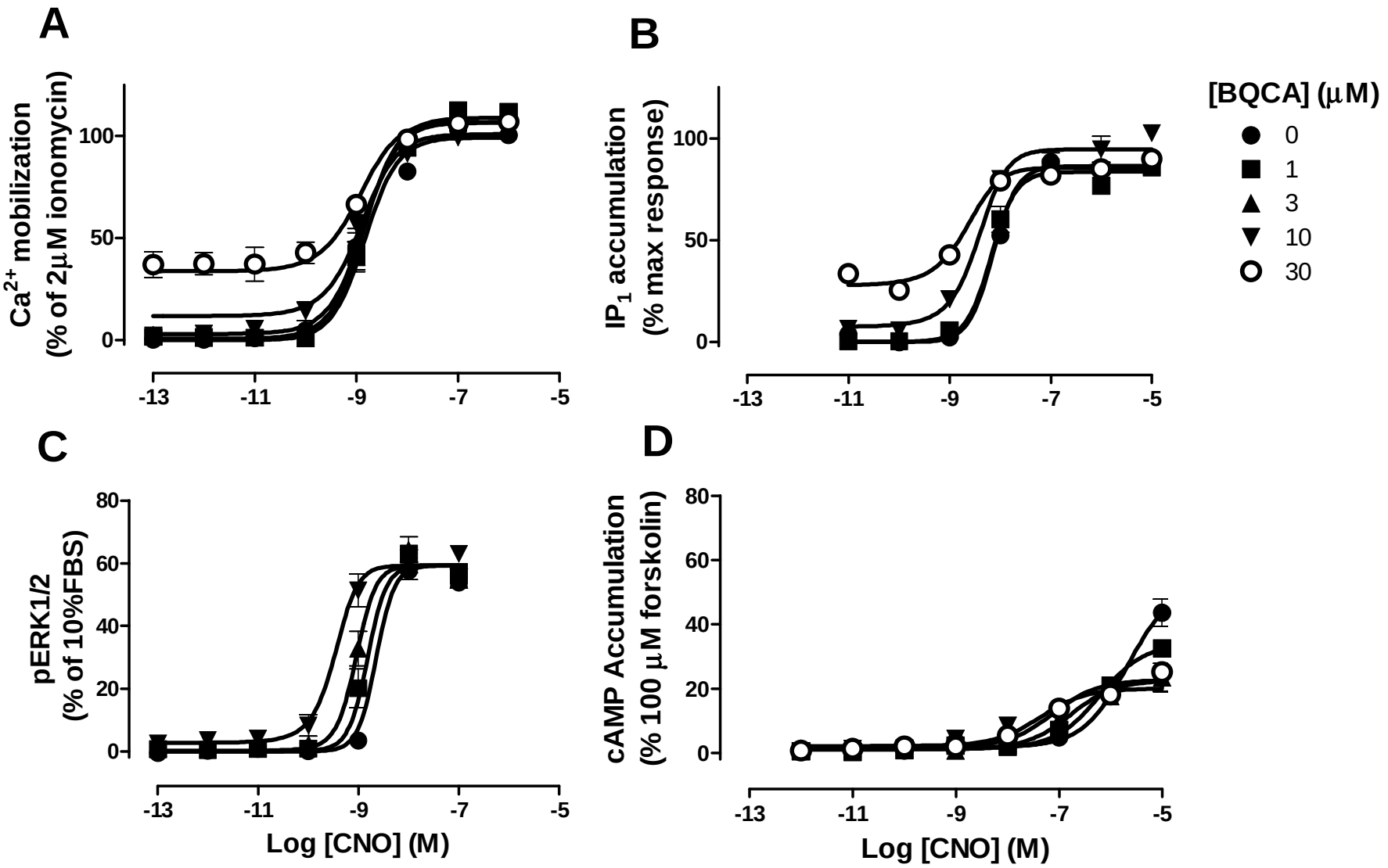

Figure 5

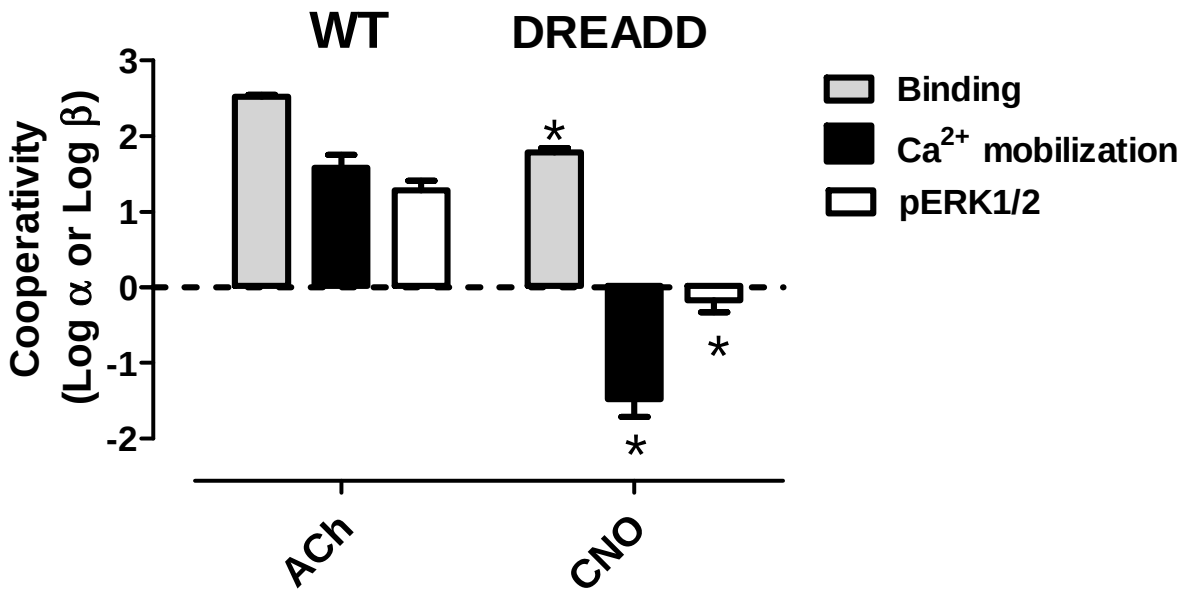

Figure 6

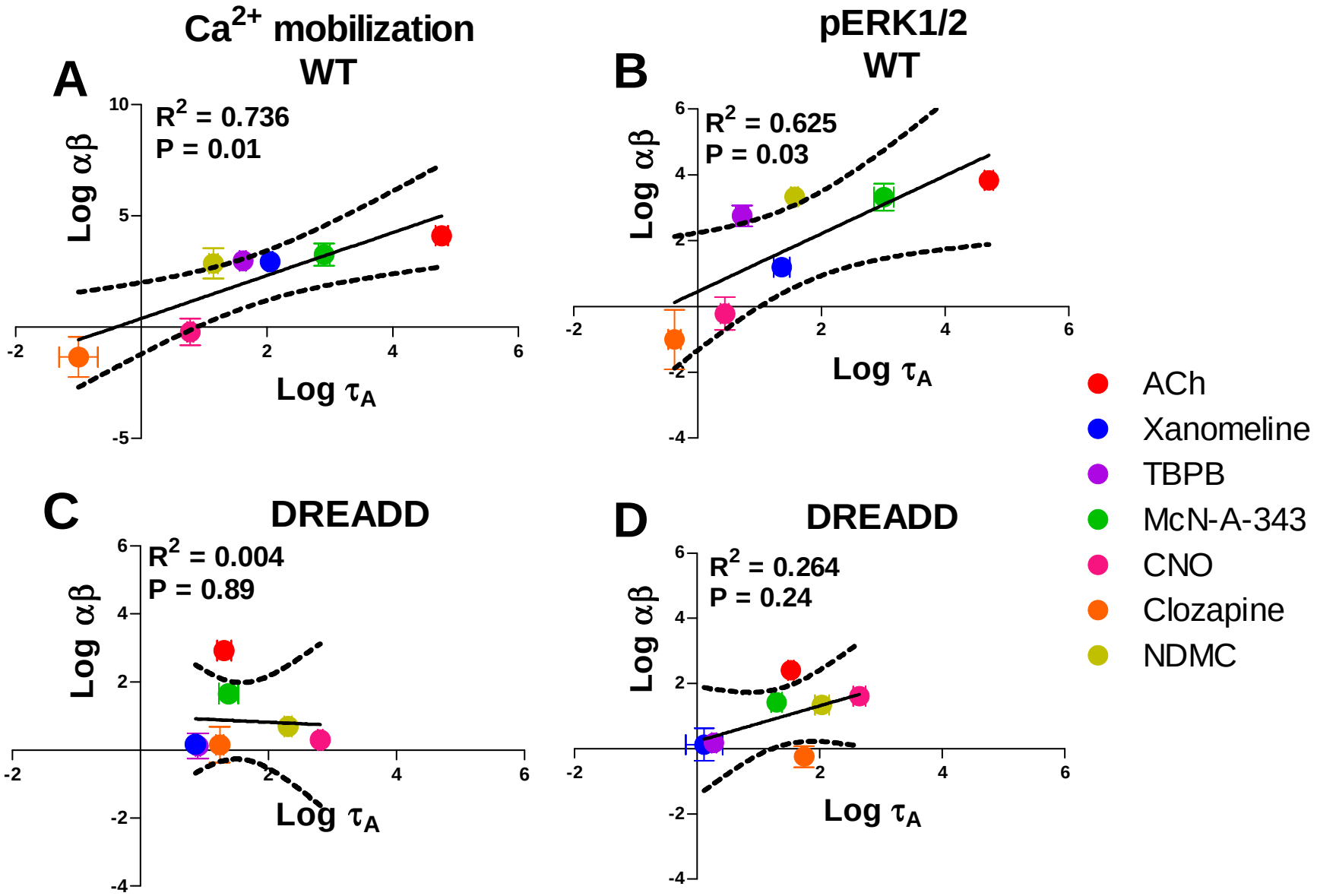

Molecular Pharmacology

Supplementary Information

Allosteric Modulation of a Chemogenetically Modified G Protein-Coupled Receptor

Alaa Abdul-Ridha, J. Robert Lane, Patrick M. Sexton, Meritxell Canals and Arthur Christopoulos

Drug Discovery Biology, Monash Institute of Pharmaceutical Sciences and

Department of Pharmacology, Monash University, Parkville, Victoria, 3052, Australia.

Supplementary Figure 1. Structures of compounds used in this study.

Supplementary Figure 2. Ligand binding properties at the M_1 WT and DREADD mAChRs. The equilibrium binding of the antagonist [^{3}H]QNB is inhibited by (A) xanomeline, (B) TBPB, (C) McN-A-343 (D) clozapine and (E) NDMC in membranes of FlpIn CHO cells expressing the WT M_1 mAChR (closed circles) and M_1 DREADD (open circles). All assays were performed using 0.13nM [^{3}H]QNB in the presence of 100μM GppNHp for 1h at 37°C. Data points represent the mean ± S.E. of three independent experiments performed in triplicate. Refer to Table 1 for parameters.

Supplementary Figure 3. Ligand receptor activation properties at the M_1 WT and DREADD mAChRs. Concentration- response curves of intracellular Ca^{2+} mobilization assays for (A) xanomeline, (B) TBPB, (C) McN-A-343 (D) clozapine and (E) NDMC in CHO FlpIn cells stably expressing the WT M_1 mAChR (closed circles) and M_1 DREADD (open circles) at 37°C. Data points represent the mean ± S.E. of three independent experiments performed in duplicate. Refer to Table 1 for parameters.

Supplementary Figure 4. BQCA's allosteric modulation of NDMC is analogous to that of CNO at the M_1 DREADD. Interaction between BQCA and NDMC in (A) [^{3}H]QNB binding inhibition assay, (B) intracellular Ca^{2+} mobilization, (C) ERK1/2 phosphorylation and (D) cAMP accumulation in CHO FlpIn cells stably expressing the M_1 DREADD mAChR. Data points represent the mean ± S.E. of three independent experiments performed in duplicate. Curves drawn through the points in (A) represent the best fit of an allosteric ternary complex model (Equation 1). Curves drawn through the points in (B and C) represent the best fit of an operational allosteric model (Equation 2).

Supplementary Table 1.

Operational model parameters for the allosteric interaction between NDMC and BQCA at the M_1 DREADD. Estimated parameter values represent the mean ± S.E from three experiments performed in duplicate and analysed according to equation 2. All other details are as for Table 3.

	Ca^{2+}	pERK1/2
Log τ_A	2.31±0.06	2.04±0.12
Log τ_B	0.31±0.06	0.24±0.18
	(2)	(1.7)
pK_B	4.05	
Log αβ (αβ)	0.70±0.21 (5)	1.35±0.26 (22)

Supplementary Table 2.

Operational model parameters for the allosteric interactions between BQCA and each of the ligands in the table in the Ca^{2+} mobilisation and ERK1/2 phosphorylation (pERK1/2) signalling pathways at the M_1 WT and DREADD mAChRs. Estimated parameter values represent the mean ± S.E from three experiments performed in duplicate and analysed according to equation 2. All other details are as for Table 3.

	Ca^{2+}				pERK1/2			
	WT		DREADD		WT		DREADD	
Ligand	Log τ_A	Log αβ	Log τ_A	Log αβ	Log τ_A	Log αβ	Log τ_A	Log αβ
ACh	4.78±0.10	4.10±0.20	1.31±0.11	2.92±0.14	4.71±0.07	3.84±0.17	1.53±0.05	2.40±0.07
Xanomeline	2.05±0.04	2.94±0.43	0.86±0.03	0.17±0.16	1.36±0.13	1.20±0.18	0.12±0.3	0.13±0.50
TBPB	1.62±0.05	2.98±0.32	0.91±0.04	0.12±0.37	0.72±0.10	2.75±0.31	0.28±0.04	0.18±0.07
McN-A-343	2.91±0.03	3.25±0.50	1.38±0.15	1.65±0.27	3.01±0.16	3.32±0.41	1.30±0.09	1.42±0.13
CNO	0.78±0.04	-0.22±0.60	2.81±0.04	0.30±0.29	0.44±0.07	-0.23±0.49	2.65±0.10	1.61±0.22
Clozapine	-1.5±0.31	-1.34±0.9	1.24±0.06	0.16±0.52	-0.37±0.10	-1.00±0.90	1.75±0.01	-0.24±0.32
NDMC	1.15±0.07	2.86±0.68	2.31±0.06	0.70±0.21	1.57±0.06	3.33±0.22	2.04±0.12	1.35±0.26

Supplementary Figure 1

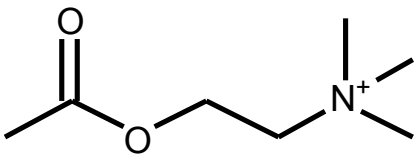

Acetylcholine

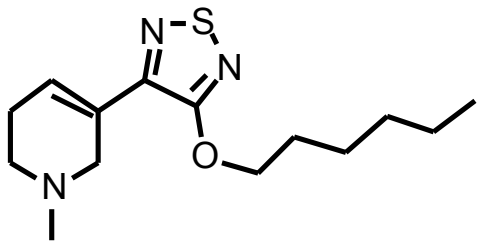

Xanomeline

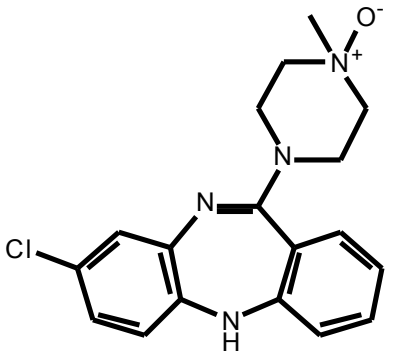

Clozapine-N-oxide (CNO)

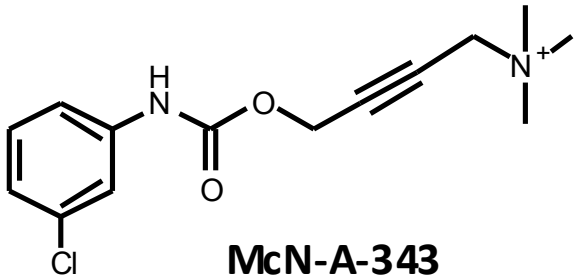

McN-A-343

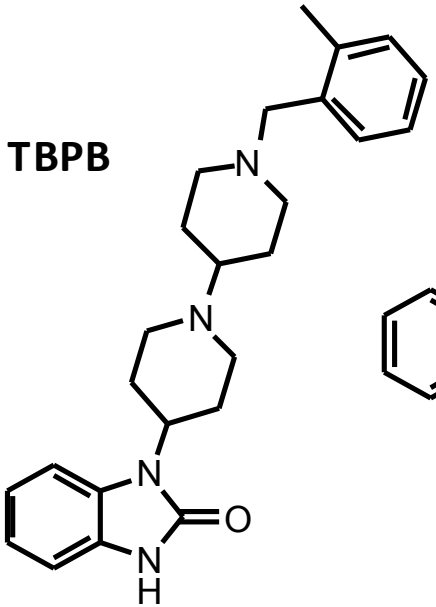

TBPB

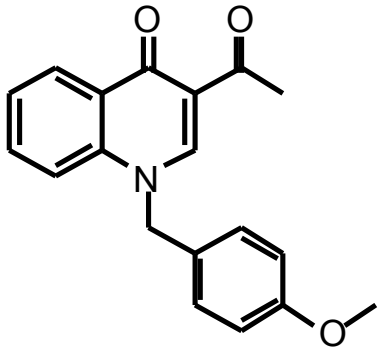

BQCA

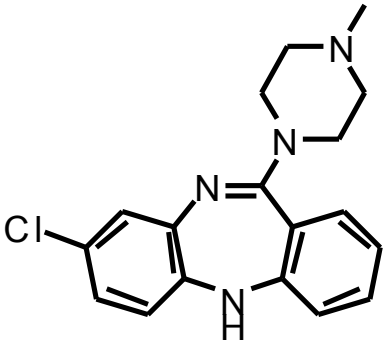

Clozapine

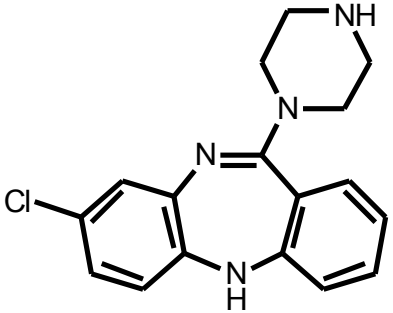

N-desmethyl clozapine (NDMC)

Supplementary Figure 2

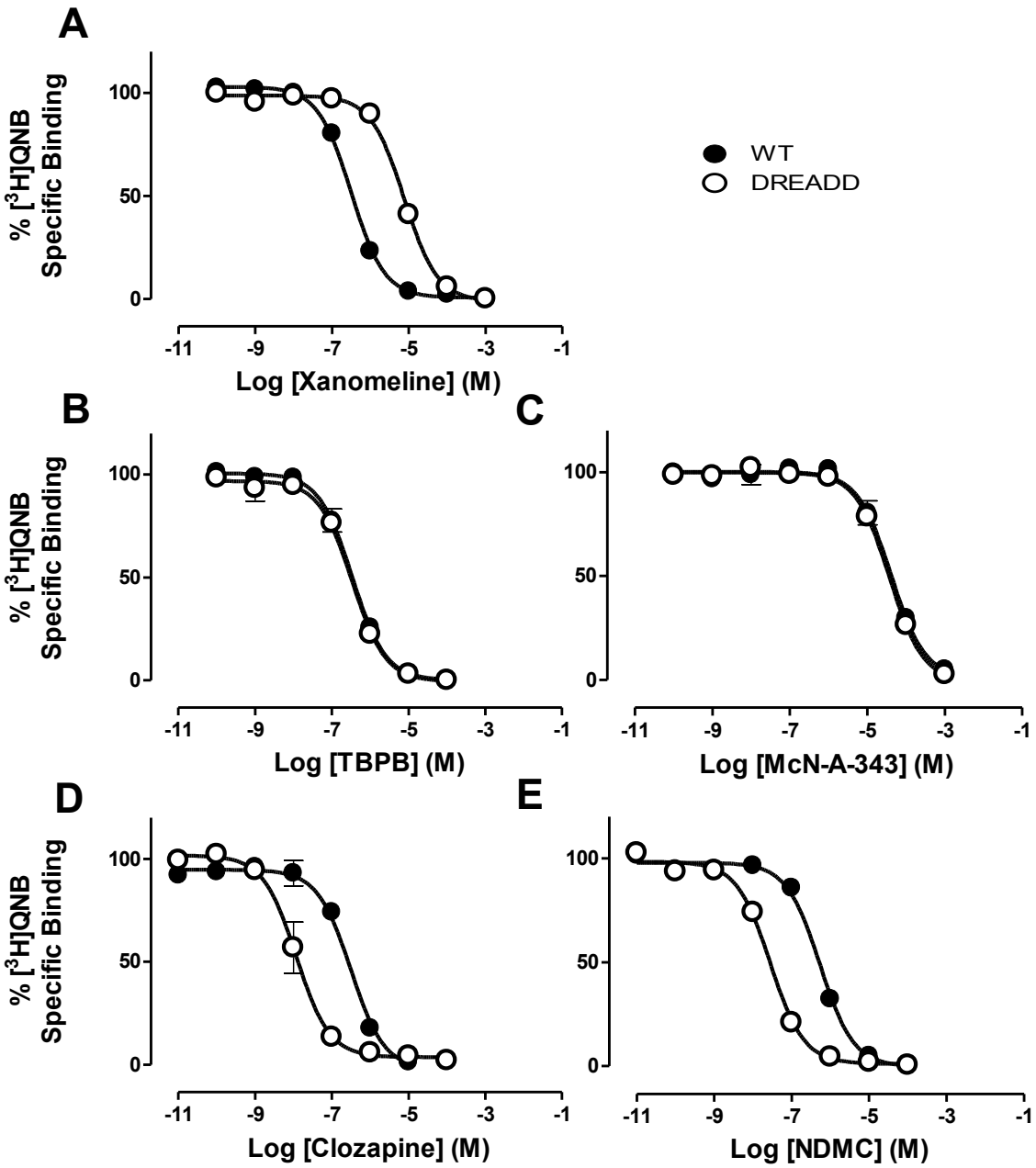

Supplementary Figure 3

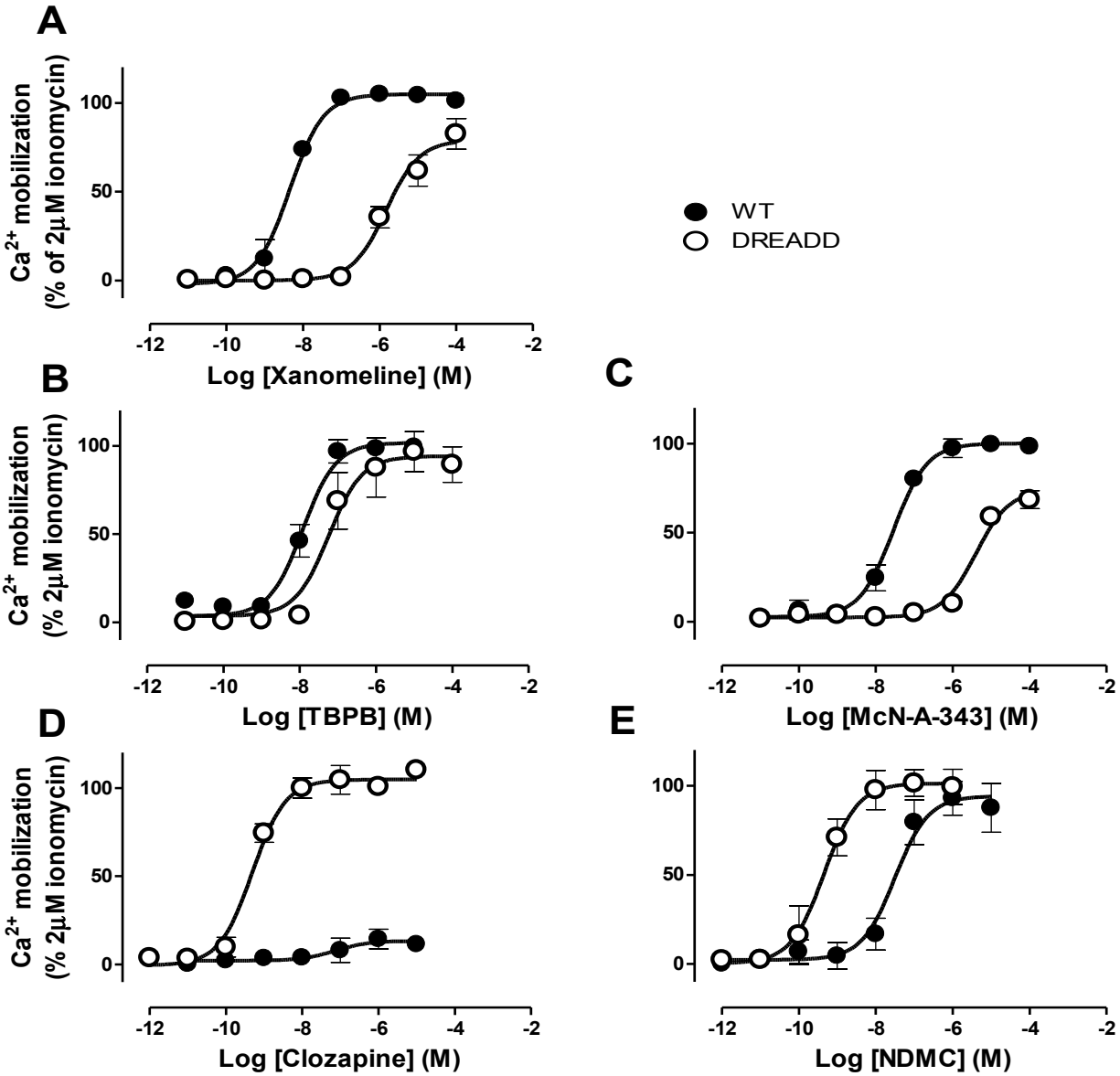

Supplementary figure 4